Int. J. of GEOMATE, Dec. 2011, Vol. 1, No. 2 (Sl. No. 2), pp. 88-94
Geotec., Const. Mat. and Env., ISSN:2186-2982(P), 2186-2990(O), Japan

Quantifying Macrodispersion in Stratified Porous Formations Using Image Processing and Spatial Moment Analysis

Katsutoshi Suzuki, Kazuya Inoue and Tsutomu Tanaka, Graduate School of Agricultural Science, Kobe University, Japan
Akira Kobayashi, Faculty of Environmental and Urban Engineering, Kansai University, Japan

ABSTRACT: Laboratory dye tracer experiments with a pulse source were conducted under saturated unidirectional flow conditions in a two-dimensional and vertically placed water tank. In tracer experiments, homogeneous and stratified porous formations, which were comprised by a few combinations with three types of soil particles, were of concern to examine the effect of variation of pore structure on macrodispersion phenomena. A new methodology using spatial moment analysis linked with image processing of a dye tracer behavior was developed to estimate macrodispersivities both in longitudinal and transverse directions. These results demonstrated that the ratio of the longitudinal macrodispersivity to the longitudinal microdispersivity ranged from about 2 to about 40. Moreover, it was indicated that the layering of stratified porous formations had an effect on the degree of longitudinal and transverse macrodispersions.

Keywords: Macrodispersion, Stratified porous media, Image processing, Spatial moment

1. INTRODUCTION

The movement of groundwater in porous media is subject to convection and dispersion, independently of any material being transported [1]. Advection and forced-advection are due to bulk movement of groundwater caused by regional movement in the aquifer and by some man-made disturbance such as pumping wells, respectively, while natural convection is relevant to differences in density. Dispersion results from the irregular movement of water in porous formations where tortuosity of flow paths is induced. On a larger scale, these irregularities are due to the presence of zones of different hydraulic conductivities. It is progressively accepted that dispersion of solutes by groundwater is governed by large-scale spatial heterogeneity of natural formations [2],[3].

The scale effect in solute transport through porous media is strongly associated with the heterogeneity and has been the topic of significant theoretical and numerical experiments. As for layered media, Güven *et al* [4] conducted deterministic analysis of dispersion in a perfectly stratified aquifer of finite thickness and suggested that the time-dependent dispersivity approached an asymptotic limit in time. Black and Freyberg [5] used Monte Carlo simulations to estimate the impact of hydraulic conductivity uncertainty on concentration uncertainty in a perfectly stratified aquifer. Fadili *et al* [6] employed a Lagrangian particle tracking to investigate the behavior of concentration and statistical moments of the transported tracer plume in multilayered media. The scale effect in solute transport in a stratified aquifer has also been studied under field conditions. Sudicky *et al* [7] observed the transitional values of both longitudinal and transverse dispersivities. Güven *et al* [8] demonstrated that the results of a single-well tracer test could be interpreted without a scale-dependent dispersivity.

Although significant work has been performed through field efforts, relatively few controlled laboratory efforts have been reported. Recently, a few of the dye tracer experiments combined with an image processing technique have been studied to quantify the behavior of dye tracers [9],[10], which have been used for a long time to trace water flow and solute movement in aquifers. McNeil *et al* [11] performed intermediate-scale laboratory experiments in heterogeneous porous media and characterized the spatial distribution of solute concentrations using image analysis methods, providing concentration distributions and longitudinal dispersivity in a corresponding porous formation. However, the variation of longitudinal and transverse macrodispersivities corresponding to the heterogeneity was not described.

The objectives of this study are to investigate the transport behavior of dye tracer in homogeneous and stratified porous formations under saturated conditions, to estimate transport parameters including the longitudinal and transverse dispersivities and dispersion coefficients and to assess macrodispersion phenomena. An image processing technique is used in conjunction with spatial moments for the reliable parameter estimation and is applied to a flow field with a layered formation.

2. TRACER EXPERIMENTS

2.1 Dye tracers and experimental apparatus

Dye tracing has been widely used to characterize water flow and solute transport behavior in porous media. Previous work demonstrated that colored dye tracers could be successfully used to visualize and monitor solute transport in a porous medium confined in a transparent container [12]. A wide variety of dye tracers such as Uranine [13],[14] and Brilliant Blue FCF [15],[16] have been utilized in geoenvironmental hydrology and have played a significant role in elucidating current understanding of the hydrological cycle and of subsurface flow and transport processes. In this study, one of the soluble dyes, Brilliant Blue FCF, was employed as a dye tracer with the initial concentration of 0.4 mg/cm^3. The specific gravity of dye tracer was 1.0001 measured using the specific gravity meter and was possible to be therefore regarded as almost the same as that of water. Although the initial concentration of dye tracer was determined to be low enough to avoid density-induced flow effects, there was no denying that the effect of gravity on solute transport during the course of movement.

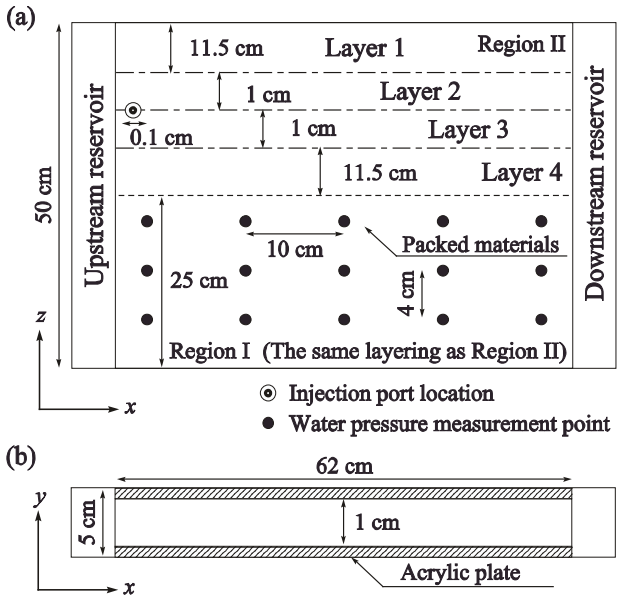

Fig.1 Schematic diagram of experimental apparatus: (a) Vertical view and (b) plane view.

Tracer experiments were carried out in a two-dimensional and vertically placed water tank with the dimensions of 62 cm width, 50 cm height and 1 cm thickness. The water flow tank allowed to contain silica sand in order to form transparent quasi two-dimensional solute transport phenomena and consisted of two acrylic plates with 2 cm thickness. Schematic diagram of experimental apparatus is shown in Fig.1. Lower and upper parts in the experimental apparatus for the measurement of the piezometric head and the observation of dye tracer transport were referred to as Region I and Region II, respectively. Constant head water reservoirs connected to the upstream and downstream ends of the water tank were used to control the hydraulic gradient. One transparent acrylic plate allowed for the observation of migrating dye tracer and for the measurement of the piezometric head at 15 observation points using manometers.

In tracer experiments, in order to elucidate the effect of the layering on the degree of macrodispersion, ten stratified porous formations were of interest and were comprised using three types of soil materials. Physical properties of soil materials, referred to as K4, K5 and K6, are shown in Table 1, as well as longitudinal and transverse microdispersivities estimated from the proposed methodology described later. For the base case, each soil material was filled in all Layers 1 through 4 shown in Fig.1 and comprised a homogeneous porous formation, providing "Single type formation" as Cases K4, K5 and K6. In two-layered porous formations, Layers 1 and 2 were filled with soil material K4 as the upper layer, while soil material K5 or K6 comprised the lower layer including Layers 3 and 4. As Cases K4-5 and K4-6, these two types of porous formations were referred to as "Step type formation". As one possible Step type formation, all three materials comprised flow fields where soil materials K4, K5 and K6

Table 1 Properties of soil materials.

	Material		
	K4	K5	K6
Mean particle size (cm)	0.085	0.050	0.030
Uniformity coefficient (-)	1.80	1.25	1.31
Hydraulic conductivity (cm/s)	0.751	0.268	0.0571
Dry density (g/cm^3)	2.68	2.68	2.68
Estimated longitudinal microdispersivity (cm)	0.175	0.163	0.127
Estimated transverse microdispersivity (cm)	0.0156	0.0153	0.0118

Table 2 Experimental cases.

Case	Layer number				Type of stratified porous formation
	1	2	3	4	
K4		K4			Single
K5		K5			Single
K6		K6			Single
K4-5	K4		K5		Step
K4-6	K4		K6		Step
K4-5-6	K4	K5		K6	Step
K4-5-4	K4	K5		K4	Convex
K4-6-4	K4	K6		K4	Convex
K5-4-5	K5	K4		K5	Concave
K6-4-6	K6	K4		K6	Concave

were filled with Layer 1, Layers 2 and 3, and Layer 4, respectively. In the same manner except for the use of two types of soil materials, soil material K4 comprised the top and bottom layers and the middle layer consisted of material K5 or K6, referred to as "Convex type formation" and as Cases K4-5-4 and K4-6-4. In Convex type formation, soil material was switched to another material in order to create two different flow fields as "Concave type formation". In Table 2, experimental cases and corresponding layering formations using three soil materials are summarized as well as the assigned name of stratified porous formations of concern.

2.2 Experimental procedure

Materials were completely washed and saturated before packing to remove organic chemicals attached to the particle surface, to avoid entering air and to conduct experiments under the saturated condition. In the process of creation of homogeneous or heterogeneous flow field formations, water flow tank was filled with water and material of interest from bottom to top in 5 cm layers to achieve uniform packing. In this process, saturated material was funneled using an extended funnel. Each layer of interest was compacted prior to filling the next layer, resulting in 0.41 of the porosity for all materials. The

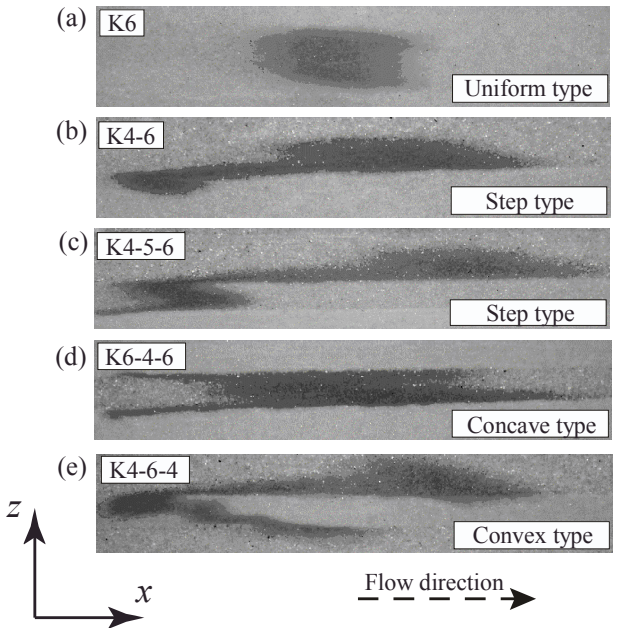

Fig.2 Representative images of dye tracer transport in each porous formation.

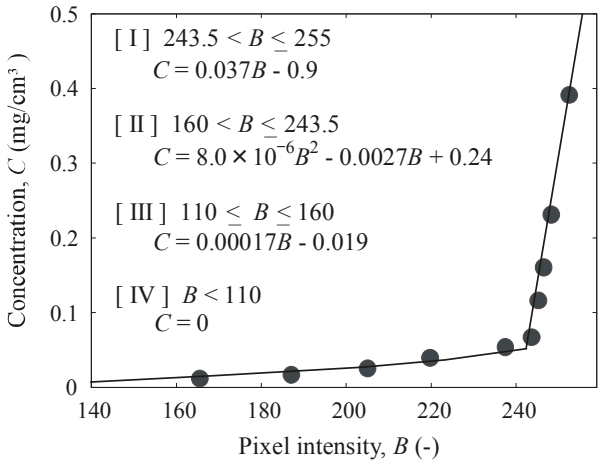

Fig.3 Relation between the pixel intensity and the dye tracer concentration.

porosity of each flow field was able to be estimated indirectly from measurements of the particle density and the dry soil bulk density.

After packing, water was applied to the flow tank under a specific hydraulic gradient controlled by constant head water reservoirs at the upstream and downstream sides, while maintaining saturated condition of porous media. A steady saturated flow field was established in the flow tank when fluctuations in the observed drainage rate, which was effluent from the constant head water reservoir, and piezometer readings at water pressure measurement points could become negligible.

After reaching steady state flow conditions, in order to simulate a pulse type source, dye tracer with the volume of 5 cm^3, which made flow paths visible, was uniformly injected along the whole thickness of the flow tank. Tracer injection required approximately 20 seconds so as not to possibly induce complications in the flow field, resulting in cylindrical source having a height of 1 cm and a radius of approximately 1.2 cm. In an injection system, a needle was inserted through the injection port with 0.05 cm of the radius on the face of acrylic plate in order to create a two-dimensional transport state. During the experiment, the profiles of tracer migration were periodically recorded using a digital camera. The distance between the digital camera and the experimental flow tank was set at approximately 40 cm. A time series of images could then be processed and analyzed through image analysis for parameter estimation. Several experimental cases were repeatedly conducted under various hydraulic gradient conditions within approximately one order range of Reynolds number. In all experiments, water temperature was in the range of 15 degree Celsius to 21 degree Celsius and varied little during a specific experimental case.

2.3 Transport process and image calibration

Figure 2 exhibits some images associated with dye tracer distributions in porous media. Each of the pixels representing an image has a pixel intensity which describes how bright that pixel is. Data recorded by the digital camera successfully indicated different pixel intensities in dye tracer distributions, suggesting different concentrations of the dye tracer. Moreover, the tracer experiments may be regarded as effectively two-dimensional since dye tracer was injected across the full 1 cm thickness of the flow tank. In order to establish the relationship between the pixel intensity of a pixel and dye tracer concentration, a calibration was conducted. Under identical experimental conditions, a known concentration of dye tracer was injected into a corresponding porous formation without a hydraulic gradient. The spread of dye was captured by the digital camera. The same procedure was repeated using different concentrations of dye tracer, providing the relation between the pixel intensity and dye tracer concentration as shown in Fig.3 where calibration formulas were also shown and were specific to the experimental configuration. Consequently, the concentration of the dye tracer as a function of the pixel intensity nonlinearly varied over the range of 0 mg/cm^3 to 0.4 mg/cm^3 as seen in Fig.3.

2.4 Spatial moment approach

A commonly used measure of dilution is the spatial moments of the concentration spatial moments of aqueous concentrations distributed in space in porous media and are calculated from snapshots of tracer plume at given times as follows [17].

$$M_{ij}(t) = \int_{-\infty}^{\infty}\int_{-\infty}^{\infty} C(x,z,t)x^i z^j dxdz \quad (1)$$

where x and z are the Cartesian coordinates, C is the solute concentration, t is the time, M_{ij} is the spatial moments associated with the distribution of tracer plume at a certain time, and i and j are the spatial order in the x and z

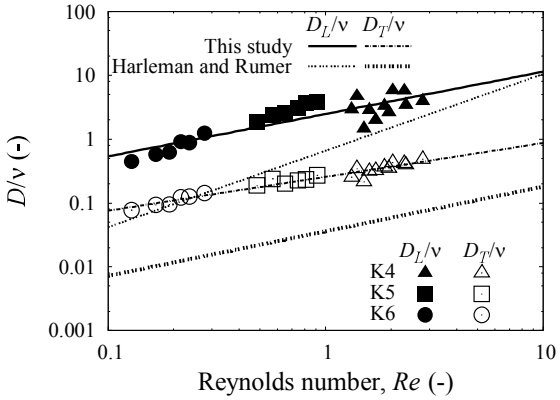

Fig.4 Variation of normalized longitudinal and transverse dispersion coefficients as a function of Reynolds number.

coordinates, respectively.

The tracer brightness distribution can be converted to a concentration distribution by the calibration, providing an analogy between Eq.(1) and Eq.(2).

$$M_{ij}(t) = \int_{-\infty}^{\infty}\int_{-\infty}^{\infty} H(x,z)B(x,z,t)x^i z^j dxdz \tag{2}$$

where $H(x,z)$ is the area per unit pixel and $B(x,z,t)$ is the intensity at a corresponding pixel.

The centroid of plume concentration distribution is calculated as the normalized first order spatial moment by the following equation.

$$x_c = \frac{M_{10}}{M_{00}}, \quad z_c = \frac{M_{01}}{M_{00}} \tag{3}$$

where x_c and z_c are the centroid locations of plume concentration distribution in the x and z coordinates, respectively. The second order spatial moments are also computed as follows.

$$\sigma_{ij} = \begin{pmatrix} \sigma_{xx} & \sigma_{xz} \\ \sigma_{zx} & \sigma_{zz} \end{pmatrix} = \begin{pmatrix} \frac{M_{20}}{M_{00}} - x_c^2 & \frac{M_{11}}{M_{00}} - x_c z_c \\ \frac{M_{11}}{M_{00}} - z_c x_c & \frac{M_{02}}{M_{00}} - z_c^2 \end{pmatrix} \tag{4}$$

where σ_{ij} is the second order spatial moments.

Longitudinal and transverse macrodispersivities from spatial moments of the distributed tracer plume are calculated as [10]

$$A_L = \frac{1}{2}\frac{\sigma_{xx}}{\xi_c}, \quad A_T = \frac{1}{2}\frac{\sigma_{zz}}{\xi_c} \tag{5}$$

where A_L is the longitudinal macrodispersivity, A_T is the transverse macrodispersivity and ξ_c is the travel distance of the center of tracer plume in the mean flow direction at a given time t .

Furthermore, the longitudinal and transverse dispersion coefficients are estimated based on the relation between the seepage velocity and the dispersivity as the following equations

$$D_L = vA_L, \quad D_T = vA_T \tag{6}$$

where D_L is the longitudinal dispersion coefficient, D_T is the transverse dispersion coefficient and v is the seepage velocity in an entire domain, which can be indirectly computed using the effluent discharge from the downstream reservoir, the porosity and the cross-section area.

An advantage of spatial moment analysis in conjunction with an image technique is that the underlying physical model is not needed unlike other techniques such as fitting advection and dispersion equation. This point may lead to the cost reduction related to labor sampling of other conservative chemicals such as NaCl and KBr.

3 RESULTS AND DISCUSSION

3.1 Microdispersion coefficient estimates

Estimates of longitudinal and transverse dispersion coefficients in single layer formations of Cases K4, K5 and K6 are shown in Fig.4 as a function of Reynolds number, which is expressed as follows [1]

$$Re = \frac{vd_{50}}{\nu} \tag{7}$$

where Re is the Reynolds number, v is the seepage velocity, d_{50} is the mean particle size and ν is the kinematic viscosity, which was performed the corrections at the temperature of 15 degree Celsius. Harleman and Rumer suggested that a nonlinear relation between dispersion coefficients and Reynolds number as follows [18]

$$D_L/\nu = b_L Re^{f_L}, \quad D_T/\nu = b_T Re^{f_T} \tag{8}$$

where b_L, b_T, f_L and f_T are constants, which depend on particle shape. The best fittings based on Eq.(8) with the empirical constants of 2.48 of b_L, 0.66 of f_L, 0.257 of b_T and 0.53 of f_T. In this figure, empirical relations suggested by Harleman and Rumer [18] were also depicted for the normalized longitudinal dispersions with the constants 0.66 of b_L and 1.20 of f_L and for the transverse dispersions with the constants 0.036 of b_T and 0.70 of f_T.

Both longitudinal and transverse dispersion coefficients increased not only with the Reynolds number in flow fields but with the mean particle size. This tendency was quite natural in solute transport phenomena in homogeneous porous media [1], indicating the validity of the methodology applied herein. On the other hand, the fitting curves obtained in this study provided larger values compared to the empirical relations because the difference between physical properties including the uniformity coefficient and the mean grain size of materials in tracer experiments employed in this study and other literature might affect a porous formation, and resulted in a wide

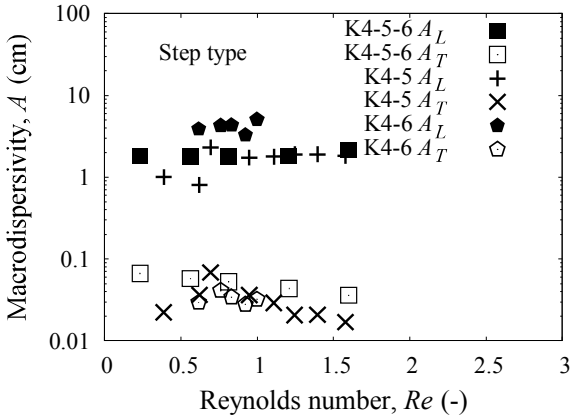

Fig.5 Variation of longitudinal and transverse macrodispersivities as a function of Reynolds number in Step type formation.

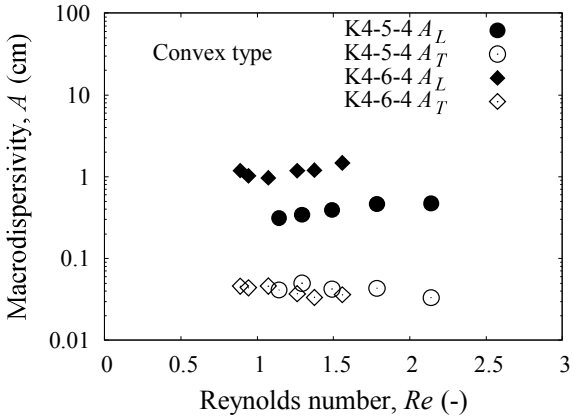

Fig.6 Variation of longitudinal and transverse macrodispersivities as a function of Reynolds number in Convex type formation.

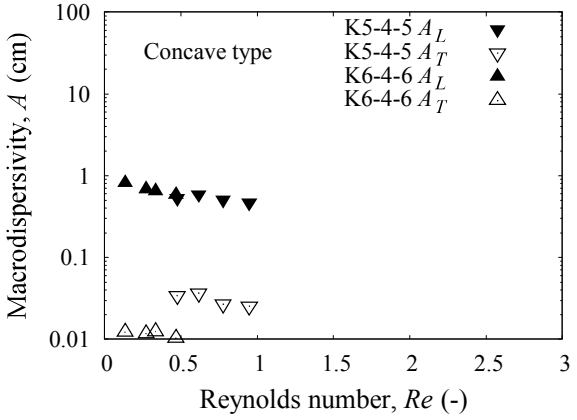

Fig.7 Variation of longitudinal and transverse macrodispersivities as a function of Reynolds number in Concave type formation.

variety of tortuous pathways during the course of tracer migration.

3.2 Macrodispersivity estimates

As stratified porous formations of Step, Convex and Concave type formations, longitudinal and transverse macrodispersivities in each formation are plotted in Fig.5 to Fig.7 as a function of Reynolds number. Longitudinal macrodispersivities in multilayered porous media were larger than those in single layers of Cases K4, K5 and K6, which were shown in Table 1. This was attributed to the distribution of hydraulic conductivity comprising flow fields and was one evidence occurring macrodispersion phenomena.

As for Step type porous formations of concern, longitudinal macrodispersivities in Case K4-6 were larger than those in Case K4-5 as shown in Fig.5. Moreover, longitudinal macrodispersivities in Case K4-5-6 were lower values than those in Case K4-6. It was inferred that larger difference of hydraulic conductivity between neighboring layers resulted in larger values of longitudinal macrodispersivity. On the other hand, the difference of transverse macrodispersivities was relatively small despite of the stratified porous formation. This was because the flow direction was parallel to the layers and the vertical component of flow velocity was almost zero in this experimental field. As for Convex type formations, the same tendency as the results of Step type formation appeared for longitudinal and transverse macrodispersivity estimates as seen in Fig.6.

On the other hand, unlike the results of Step and Convex type formations, Concave type formations where the soil material having the largest hydraulic conductivity comprised the middle layer in three layers presented a unique tendency as shown in Fig.7. Whereas a little difference of the longitudinal macrodispersivity estimates between Cases K5-4-5 and K6-4-6 appeared, transverse macrodispersivity estimates depended on the soil materials comprising the top and bottom layers. A few studies [19], [20] mentioned a solute transfer across a discontinuity such as a layered formation and suggested a probability expression as follows

$$P_1 = \frac{\sqrt{D_1}}{\sqrt{D_1} + \sqrt{D_2}} \tag{9}$$

$$P_2 = 1 - P_1 = \frac{\sqrt{D_2}}{\sqrt{D_1} + \sqrt{D_2}} \tag{10}$$

where D_1 is the transverse dispersion coefficient in a layer in which tracer exists, D_2 is the transverse dispersion coefficient in the neighbor layer, P_1 is the transfer probability that a tracer remains in the same layer in which tracer exists and P_2 is the transfer probability that a tracer goes into the neighboring layer.

Eq.(9) and Eq.(10) can be expressed as follows

$$P_1 = \frac{\sqrt{\alpha_T^1 K_1 I_1 / n_1}}{\sqrt{\alpha_T^1 K_1 I_1 / n_1} + \sqrt{\alpha_T^2 K_2 I_2 / n_2}} \tag{11}$$

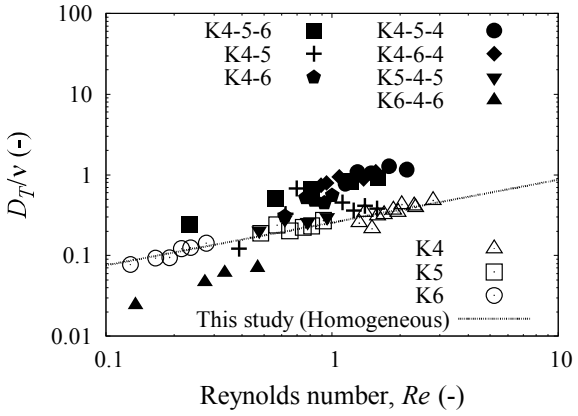

Fig.8 Variation of normalized transverse dispersion coefficients as a function of Reynolds number.

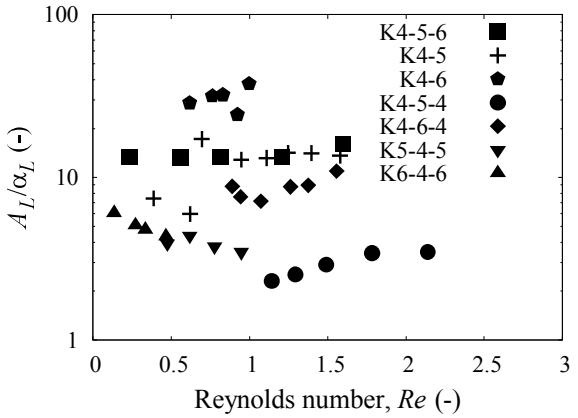

Fig.9 Variation of normalized longitudinal macrodispersivities as a function of Reynolds number.

$$P_2 = \frac{\sqrt{\alpha_T^2 K_2 I_2 / n_2}}{\sqrt{\alpha_T^1 K_1 I_1 / n_1} + \sqrt{\alpha_T^2 K_2 I_2 / n_2}} \quad (12)$$

where α_T^i is the transverse microdispersivity in each layer i, K_i is the hydraulic conductivity in each layer i, I_i is the hydraulic gradient in each layer i and n_i is the porosity in each layer i. In this study, each layer had the same porosity under the same hydraulic gradient condition. Hence, the following equations can be obtained.

$$P_1 = \frac{\sqrt{\alpha_T^1 K_1}}{\sqrt{\alpha_T^1 K_1} + \sqrt{\alpha_T^2 K_2}} \quad (13)$$

$$P_2 = \frac{\sqrt{\alpha_T^2 K_2}}{\sqrt{\alpha_T^1 K_1} + \sqrt{\alpha_T^2 K_2}} \quad (14)$$

As seen in Table 1, Case K4 had the largest values of transverse microdispersivity and hydraulic conductivity among flow fields of Single type formation. In addition, the values of transverse microdispersivity exhibited a tendency to become smaller in soil material, which has smaller hydraulic conductivity. Therefore, according to the expression of Eq.(13) and Eq.(14), tracers migrating in the K5 or K6 layer had a tendency to travel toward the K4 layer. Hence, as shown in Fig.7, in Concave type porous formations employed herein, it appeared that the difference of hydraulic conductivity between layers had no effect on the variation of longitudinal macrodispersivity estimates but on transverse macrodispersivity estimates.

3.3 Macrodispersivity vs. microdispersivity

As for results in stratified porous formations, Fig.8 exhibits the variation of the transverse macrodispersion coefficient as a function of Reynolds number. Additionally, for the purpose of comparison between macrodispersion and microdispersion coefficient estimates, transverse dispersion coefficients in Single type formation in Cases K4, K5 and K6 were also plotted. Transverse macrodispersion coefficient estimates in Step and Convex type formations were larger than those estimated in single layers K4, K5 and K6. This was because tracers migrating in K5 or K6 layer might tend to flow into the K4 layer as aforementioned above. Opposite to this result, transverse macrodispersion coefficient estimates in the Concave type formation of Case K6-4-6 were smaller than those estimates in single layers K4, K5 and K6. This also attributed to the difference of hydraulic conductivity between two layers. In Concave type formations, tracers located in the top and bottom layers had a certain possibility to flow into the middle layer, which has the largest hydraulic conductivity. Therefore, the degree of transverse dispersion showed a tendency to decrease as tracers move.

However, as shown in Fig.8, one of the Concave type formations, Case K5-4-5, provided almost the same values of transverse macrodispersion coefficients as those in Single type formations. According to Eq.(9) to Eq.(14), the transfer possibility of tracers depends on the transverse dispersivity. There was a small difference between not only transverse dispersivities but the values of hydraulic conductivity in soil materials K4 and K5, resulting in similar values of Case K5-4-5 to the results of Single type formation.

Figure 9 demonstrates that the variation of the longitudinal macrodispersivities divided by the microdispersivity (α_L=0.175cm), which was an estimate in Single type formation of Case K4, as a function of Reynolds number. Regardless of stratified porous formations, the ratio of the longitudinal macrodispersivity to the longitudinal microdispersivity exceeded 1, and ranged from about 2 to about 40. Moreover, there was a marked difference between estimated values of A_L/α_L in stratified porous formations. In Step type formation the values of A_L/α_L were larger than those in Convex and Concave type formations due to the difference of the degree of transverse dispersion induced from the layering comprising stratified formations.

4 CONCLUSION

In the present study, the behavior of macrodispersion in stratified porous formations was assessed. Macrodispersion coefficient and microdispersivity were estimated based on

spatial moments in conjunction with image processing. The following findings were clarified.

1. Image processing was a non-intrusive approach and was able to directly characterize the solute movement in porous media.
2. Transverse macrodispersion coefficient estimates in Step and Convex type formations were larger than those in Single type formations. Contrary tendency was seen in Concave type formation due to the effect of the layering comprising stratified formations.
3. Regardless of stratified porous formations, the ratio of the longitudinal macrodispersivity to the longitudinal microdispersivity exceeded the unity, and ranged from about 2 to about 40.
4. The layering of stratified porous formations had a significant impact on longitudinal and transverse macrodispersion.

5 REFERENCES

[1] Bear J, Dynamics of fluids in porous media. Dover Publications.

[2] Dagan G, "Time-dependent macrodispersion for solute transport in anisotropic heterogeneous aquifers," Water Resour. Res., 24(9), 1988, pp. 1491–1500.

[3] Gelhar LW, Welty C and Rehfeldt KR, "A critical review of data on field-scale dispersion in aquifers," Water Resour. Res., 28(7), 1991, pp. 1955–1974.

[4] Güven O, Moltz, JM and Melville JG, "An analysis of dispersion in a stratified aquifer," Water Resour. Res., 20(10), 1984, pp. 1337–1354.

[5] Black TC and Freyberg DL, "Stochastic modeling of vertically averaged concentration uncertainty in a perfectly stratified aquifer," Water Resour. Res., 23(6), 1987, pp. 997–1004.

[6] Fadili A, Abaou R and Lenormand R, "Dispersive particle transport: identification of macroscale behavior in heterogeneous stratified subsurface flows," Math. Geol., 31(7), 1999, pp. 793–840.

[7] Sudicky EA, Cherry JA and Frind EO, "Migration of contaminants in groundwater at a landfill: a case study 4. A natural-gradient dispersion test," J. Hydrol., 63, 1983, pp. 81–108.

[8] Güven O, Falta RW, Moltz, JM and Melville JG, "Analysis and interpretation of single-well tracer test in stratified aquifers," Water Resour. Res., 21(5), 1985, pp. 676–684.

[9] Schincariol R and Schwartz FW, "An experimental investigation of variable density flow and mixing in homogeneous and heterogeneous media," Water Resour. Res., 26(10), 1990, pp. 2317–2329.

[10] Inoue K, Takenouti R, Kobayashi A, Suzuki K and Tanaka T, "Assessment of a UV excited fluorescent dye technique for estimating solute dispersion in porous media," J. Rainwater Catchment Systems, 17(1), 2011, pp. 1–9.

[11] McNeil JD, Oldenborger GA and Schincariol RA, "Quantifying imaging of contaminant distributions in heterogeneous porous media laboratory experiments," J. Contam. Hydrol., 84, 2006, pp. 36–54.

[12] Flury M and Flühler H, "Tracer Characteristics of Brilliant Blue FCF," Soil Sci. Soc. Am. J., 59(1), 1995, pp. 22–27.

[13] Hoehn E and Santschi PH, "Interpretation of tracer displacement during infiltration of river water to groundwater," Water Resour. Res., 23(4), 1987, pp.633-640.

[14] Mikovari ACP and Leibundgut Ch, "Investigation of preferential flow using tracer techniques," In: Tracer Technologies for Hydrological Systems, Proc. Boulder Symposium, IAHS Publ. 229, 1995, pp.87-97.

[15] Flühler H, Durner W and Flury M, "Lateral solute mixing processes - a key for understanding field-scale transport of water and solutes, " Geoderma, 70, 1996, pp.165-183.

[16] Inoue K, Masaki I, Setsune N and Tanaka T, "Tracer experiments and parameter estimation in horizontally two-dimensional homogeneous porous media, " Trans. Jpn. Soc. Irrig. Drain. Reclam. Eng., 74(1), 2006, pp.87-95.

[17] Tompson AFB and Gelher LW, "Numerical simulation of solute transport in three-dimensional, randomly heterogeneous porous media," Water Resour. Res., 26(10), 1990, pp. 2541–2562.

[18] Harleman DRF and Rumer RR, "Longitudinal and lateral dispersion in an isotropic porous media," J. Fluid Mech., 16, 1963, pp. 385–394.

[19] Hoteit H, Mose R, Younes A, Lehmann F and Ackerer P, "Three-dimentional modeling of mass transfer in porous media using the mixed hybrid finite elements and the random-walk methods," Math. Geol., 34(4), 2002, pp. 435–456.

[20] Uffink GJM, "A random-walk method for the simulation of macrodispersion in a stratified aquifer," Proc. IAHS symposia, 65, 1985, pp. 26–34.

International Journal of GEOMATE , Dec. 2011, Vol. 1, No.2 (Sl. No. 2) MS No. 2f received Dec.8, 2011, and reviewed under GEOMATE publication policies.

Corresponding Author: Kazuya Inoue